Translational Research in Anatomy 16 (2019) 100047

Contents lists available at ScienceDirect

Translational Research in Anatomy

journal homepage: www.elsevier.com/locate/tria

The organisation of vascular smooth muscle cells; a quantitative Fast Fourier Transform (FFT) based assessment

Cristina Garcia Cordoba, Craig J. Daly*

School of Life Science, College of Medical, Veterinary & Life Sciences, University of Glasgow, Glasgow, G128QQ, United Kingdom

ARTICLE INFO

Keywords:
Confocal laser scanning microscopy (CLSM)
Image analysis
Vascular anatomy
Artery
Fast Fourier Transform (FFT)

ABSTRACT

Background: The existence of a helical arrangement of vascular smooth muscle cells in the wall of relatively large blood vessels has been known of for at least 80 years. In that time various workers have proposed mathematical models of vascular function that have incorporated one or more helix. However, most of this work has focussed on large conduit vessels such as aorta and carotid arteries. The smaller resistance arteries are more difficult to study and do not have such an apparent helical arrangement, although there are suggestions of its existence in the patterning of smooth muscle cells in the tunica media.

Method: We have employed confocal laser scanning microscopy (CLSM) and a relatively simple Fast Fourier Transform (FFT) based image analysis method to examine a collection of extended focus (z-projection) images of the tunica media of mouse superior mesenteric artery. A fluorescent nuclear stain (Syto 61) was used to identify smooth muscle cell orientation and arrangement. Thirty-six CLSM datasets representing the tunica media of mesenteric arteries taken from 12 C57/black mice were collected for analysis.

Results: Measurements of Z-projection (extended focus) images, of the tunica media, were compared with measurements made on inverse FFT images where the high frequency information was removed. The results, of both measurement types, indicated the existence of an underlying basic helical arrangement of cells that has a pitch angle of 49°. 3D electron microscopy-based models of individual smooth muscle cells (from the tail artery) were generated to highlight their heterogeneity and orientational position within the tunica media.

Conclusion: Inverse FFT images provide a more objective means of measuring cell organisation and therefore could be used in automated processes. Whilst we propose the existence of an underlying helical arrangement of smooth muscle cells, we do not discount the existence of other helices each with different angles, but these may be more difficult to detect and may extend radially (deep within the tunica media) as well as longitudinally.

1. Introduction

The observation that the arteries of hypertensive patients are changed stretches back to the late 1800's. Possibly the first identification of hypertension-induced arterial thickening comes from the beautiful hand drawn plates in a paper by Gul & Sutton in 1872 [1]. Although this paper focusses on kidney disease, the diagrams of vascular structure, showing a thickened tunica media, are extremely familiar as 'remodelled' arteries. Although not stated at the time, this may be the first identification of hypertensive nephrosclerosis. Similar vascular observations appear in the work by David Short from 1957 to 1966 [2] in which the important physiological relationship between wall thickness and lumen diameter begins to emerge. It is interesting that in Short's paper [2] he describes vascular remodelling which does not involve hypertrophy or hyperplasia but acknowledges there are some cases that do. '*If the increased wall/lumen ratio does not indicate hypertrophy or hyperplasia, what is the significance*?' [2]. We now know the significance is that smooth muscle cells (SMCs) are not changing their shape, size or number, but their arrangement changes. It is more likely that there is a remodelling of the existing cellular and extracellular material [3]. Eventually, around 20 years ago, it became clear that vascular remodelling could take many different forms depending on the direction in which the lumen remodelled (inward or outward) and whether the tunica media exhibited changes in cellular growth or number [4]. From this, it is logical to assume that if remodelling can be so readily identified then normal vascular structure must be fairly well described. However, it is not.

The typical textbook description of vascular smooth muscle is of '*spindle shaped cells, 20-60 μm long by ~4 μm wide, wrapped helically around the vessel*' [5]. This is evident in arterioles comprising only one

* Corresponding author.
E-mail address: craig.daly@glasgow.ac.uk (C.J. Daly).

https://doi.org/10.1016/j.tria.2019.100047
Received 5 February 2019; Accepted 10 August 2019
Available online 13 August 2019

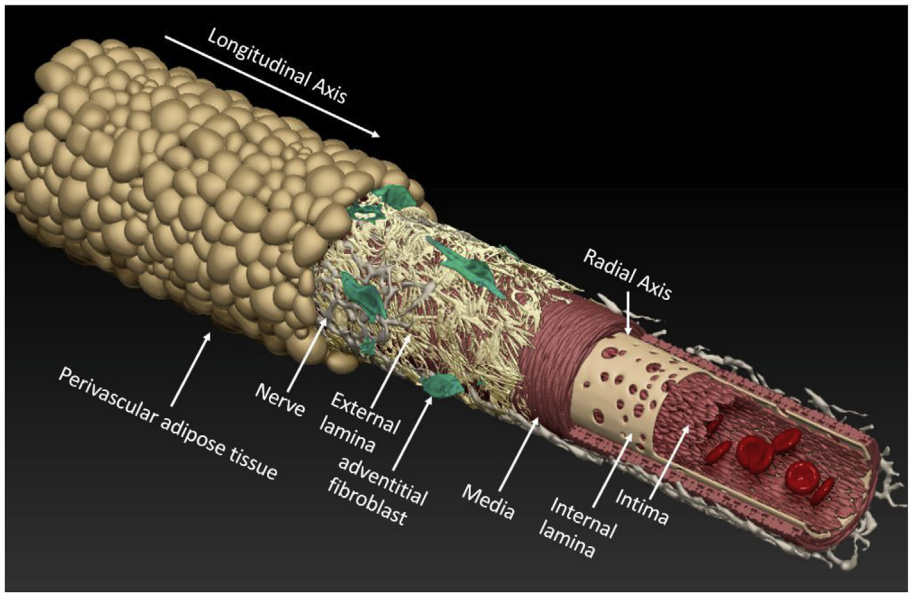

Fig. 1. The normal 'textbook-style' structure of an artery. Most of the structures in the diagram are derived from (or are based on) confocal laser scanning microscope (CLSM)-derived data. Perivascular adipocytes are CLSM derived but are duplicated for completeness. Internal elastic lamina is CLSM derived. Adventitial cells (green) are CLSM derived fibroblasts. The tunica media is an artist's impression. The tunica intima is constructed from a small number of CLSM-derived endothelial cells. Red blood cells are drawn. The diagram is a hybrid model of real and imagined structures. (For interpretation of the references to colour in this figure legend, the reader is referred to the Web version of this article.)

SMC layer. 3D anatomical investigations have demonstrated the helical orientation of each SMC in which at least two morphologies (round and spindle) are identified [6]. In larger arteries (i.e. tail, femoral and mesenteric) the SMCs have been reported to assume a multitude of elongated shapes with varying orientations [7]. However, there has been less attention paid to identifying patterns of cellular arrangement. If single cells (in very small vessels) have a spiral orientation, are groups of cells also arranged in a helical fashion? The existence of such an underlying basic pattern of SMC arrangement has been suggested in small resistance arteries (i.e. mesenteric artery) [8]. Multiple SMCs arranged in an underlying helical fashion makes some sense and can be clearly observed in mouse and rat mesenteric arteries [8 and 9]. A helical pattern of smooth muscle cells has, more recently, been identified in the pocine aorta [10] and mouse carotid artery [11]. The studies on large blood vessels [10 and 11] employed the use of sophisticated image analysis and mathematical modelling. We previously proposed Fast Fourier Transform (FFT) analysis as a relatively simple means of identifying any underlying patterns of SMC arrangement [8 and 9]. Therefore, in the present study we returned to this method to assess its usefulness in identifying any underlying (expected) helical pattern of smooth muscle cell arrangement in mouse mesenteric artery. In addition, we use an 840-slice electron microscope-derived image volume to describe the true shape and orientation of single smooth muscle cells.

Therefore, the aims of the current study are to build on our previous observations and.

i) Propose a working hypothesis of vascular SMC arrangement in the mouse mesenteric artery using an FFT-based analysis.
ii) Assess (and discuss) the general usefulness of FFT analysis in quantifying cellular patterns in blood vessels by comparing measurements made on original images versus inverse FFT images.

In addition, we provide further supporting evidence for the orientation of individual SMCs using a 3D reconstruction of serial electron microscopy images.

2. Material and methods

2.1. Animals

12 male mice (C57-black) with a mean weight of 31.93g (± 3.29 g s.d.) and mean age of 6.3 months (± 1.78 s.d.) were killed by CO2 inhalation followed by bleeding via the femoral artery. Immediately post-euthanasia, the section of intestines from the proximal portion of the duodenum to the distal colon were removed from the abdominal cavity and placed into a petri dish containing physiological salt solution (PSS). Tails were removed from a sub-group of mice. Animals were bred in house at the University of Glasgow, Central Research Facility. Animals were housed and fed under normal procedures complying with all local veterinary and ethical legislations.

2.2. Dissection

The superior mesenteric artery (SMA) was located branching off from the abdominal aorta and proximal to the small intestine and cecum. The perivascular adipose tissue enclosing the superior mesenteric artery and vein was removed, and the SMA was extracted and transferred into another petri dish containing PSS. Tails were marked on their underside prior to removal and pinned in a petri-dish containing PSS. The skin was cleared, and the proximal half of the artery removed to fresh PSS.

2.3. Chemicals and reagents

Physiological salt solution (PSS) contained the following: sodium chloride (119 mM), potassium chloride (4.70 mM), magnesium sulphate (1.20 mM), sodium bicarbonate (24.90 mM), potassium di-hydrogen orthophosphate (1.20 mM), calcium chloride (2.5 mM), glucose (11.1 mM). PSS was made in deionized water; and bubbled with 95% oxygen/5% Carbon dioxide to pH 7.4, at 37 °C. Collagenase and elastase were from Sigma Aldrich, UK; Syto 61 and DiIC18(3)-DS was from Thermo Fisher Scientific, UK.

2.4. Tissue staining

The arterial samples were first treated with collagenase (0.5 mg/ml) and elastase (0.25 mg/ml) for 10 min at 37 °C to remove the tunica adventitia from the arterial wall and facilitate the staining of the tunica media. Subsequently, two fluorescent stains: Syto 61 far-red fluorescent nuclear stain (5 mM) and DilC18 (3)-DS yellow fluorescent cell membrane and lipid stain (10 mM) were used to enable the detection and visualization of vascular SMCs (VSMCs) using a BioRad Radiance 2100 Confocal Laser Scanning Microscope (CLSM). The arterial samples were incubated in the staining mix in the dark for 30 min at 21 °C (room

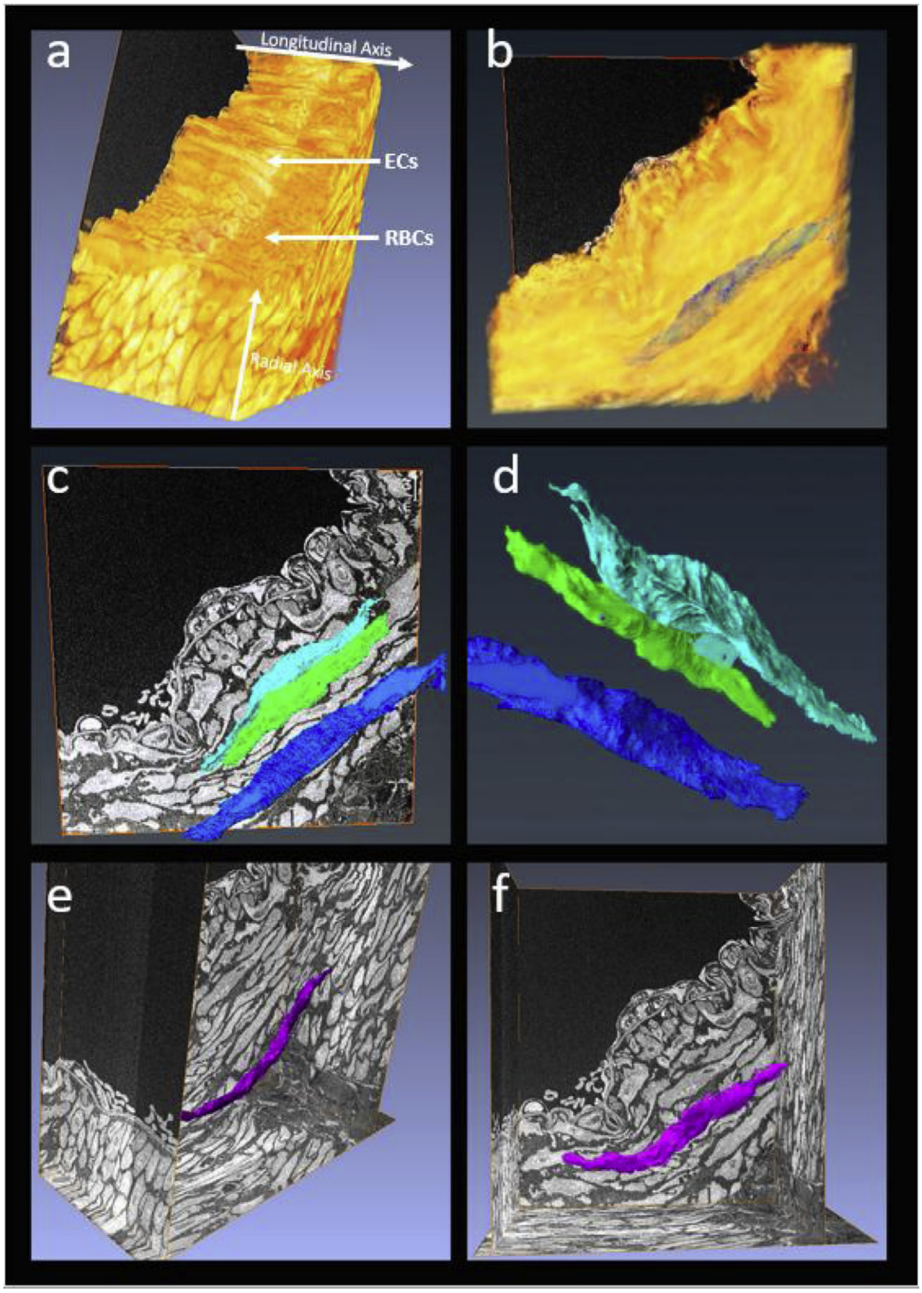

Fig. 2. Segment of mouse tail artery section using a Gatan 3View TEM. The dataset is comprised of 840 sections (70 nm spacing) and depicts the inner luminal surface and tunica media. a) The full dataset has been volume rendered in AMIRA. Smooth muscle cells are seen in cross section in the bottom left portion of the volume. Red blood cells (RBCs) can be seen resting on the endothelial cells (ECs) of the tunica intima. b) As the opacity in the volume rendering is reduced, the position of individual (segmented) smooth muscle cells begins to emerge. c&d) three flat elongated smooth muscle cells are oriented with their narrow edges facing towards the luminal surface. The flat surfaces are therefore aligned longitudinally, parallel to the axis of flow (i.e not flat side down on the lumen). e&f) a single smooth muscle cell from within the tunica media positioned to show the orientation of the narrow and flat faces. Size bars are not shown due to the varying viewpoints. However, the data volume measures 154 × 154 × 58.8 μm. (For interpretation of the references to colour in this figure legend, the reader is referred to the Web version of this article.)

temperature) and then for 60 min at 5 °C. One sample of mouse tail artery was kindly processed by Gatan for sectioning in their 3View (3D TEM) system.

2.5. Image capture

12x SMA samples were visualised on a CLSM (Radiance 2100) which housed three lasers: far red (637nm/660 nm (ex/em)), green (488nm/515 nm) and red (543nm/570 nm). An oil immersion 40x objective was used and the scan size was 512 × 512 pixels. The field of view of each image was 263.42 × 263.42 μm. From each of the 12 arterial samples, 3 randomly selected fields of view (FOV) were selected for image acquisition for a total of 36 sites. The sites were chosen using a random (online) number generator [12] to generate *x* and *y* Vernier coordinates on the microscope stage. A z-series of optical sections (a set of axial-aligned images) was taken through the depth of the tunica media at each FOV between both elastic lamina (external and internal), using Lasersharp 2000 software (Bio-Rad Laboratories Inc, UK). The step size between each optical section was 0.5 μm.

2.6. Image processing

ImageJ software (National Institute of Health, USA) was employed for all confocal analysis. For each set of images obtained using the CLSM, only the sections which contained the tunica media were selected. The images were then merged into a single image (average intensity projection) using the z-projection function at average intensity, for a total of 36 stacked images (FOVs). (The 2D z-projection images are referred to as 'original' from this point to distinguish them from their inverse-FFT partner images). Due to the difficulty in accurately visualising where the VSMC membrane ends, the nuclei were selected to represent the cell since the nucleus is normally located in the centre (or widest part) of the cell in both longitudinal and transverse axes [13] and it follows the position, orientation and arrangement of the whole cell [9]. The 'threshold' function was used to select only the nuclei from the z-projection image prior to 'segmenting' to produce a binary image.

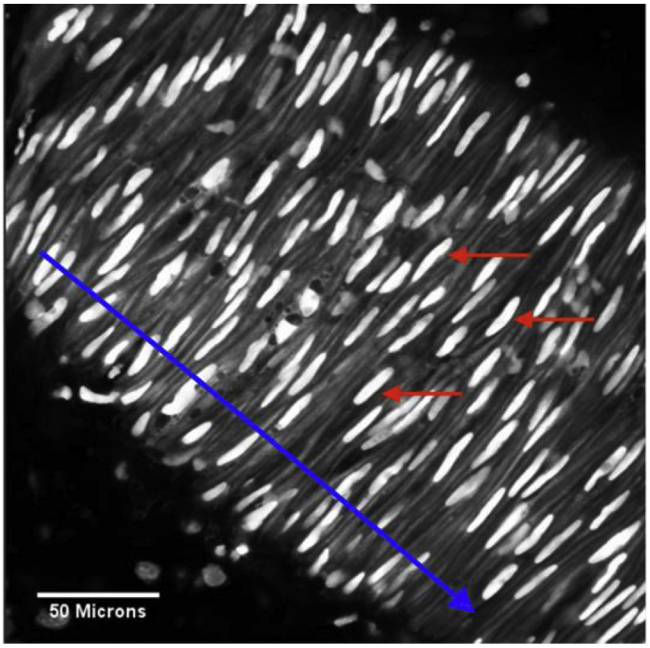

Fig. 3. Average intensity projection of the tunica media of a mouse mesenteric artery, merged from 15 images using the image J Z-project function. The artery is observed running diagonally in the image. The blue arrow represents the longitudinal axis (length) of the artery and the red arrows point to the nuclei of VSMCs within the tunica media. Size bar 50 µm. (For interpretation of the references to colour in this figure legend, the reader is referred to the Web version of this article.)

The 'open' binary function was then used to remove single pixels.

2.7. 3D reconstruction software

3D volumetric rendering of CLSM z-series data was performed in AMIRA. The thresholding and segmentation routines in AMIRA were used to isolate the individual smooth muscle cells from the 3D TEM (Gatan) data set. Vascular structure models and helical coils were created in Autodesk MAYA.

2.8. Pattern analysis

Once the threshold and open binary function had been applied, the Fast Fourier Transform (FFT) function was used to convert an image from the spatial domain to the frequency domain. A threshold was used to select the brightest, most central, hence 'low frequency', points. Subsequently, the image was inverted back into the spatial domain by applying the inverse FFT tool. The resulting image is referred to as the inverse FFT image. This image displays any fundamental (low frequency) pattern in the image without strong and bright (high frequency) detail.

2.9. Angle measuremen

From a 2D perspective, any helix created by VSMCs arrangement would be seen as a diagonal chain of VSMC nuclei that are aligned at approximately the same angle around the circumference of the vessel and positioned next to each other but with a relative offset on the longitudinal and transverse (circular) axis. This flat view of a helix would have the appearance of a sine wave or diagonal lines. To measure

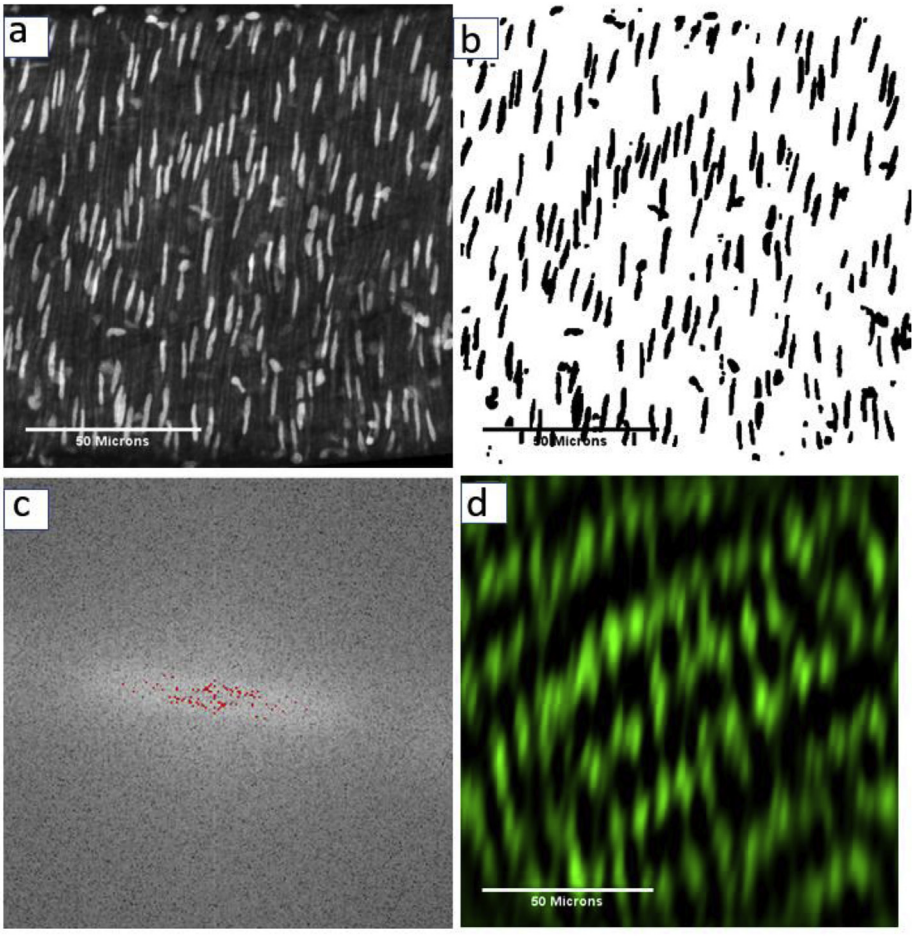

Fig. 4. A series of Image processing functions used to allow pattern analysis of the vascular smooth muscle cell (VSMC) arrangement in the artery wall. a) original image where the nuclei of VSMCs is shown in white. b) binary (segmented) image of the nuclei alone in (a) after applying threshold and open binary function. c) shows the low frequencies of the FFT plot selected (in red). d) 'inverse FFT' of low frequency (selected) data. The inverse FFT shows a series of diagonal chains, that may represent an underlying helix from a 2D perspective. Size bar 50 µm. (For interpretation of the references to colour in this figure legend, the reader is referred to the Web version of this article.)

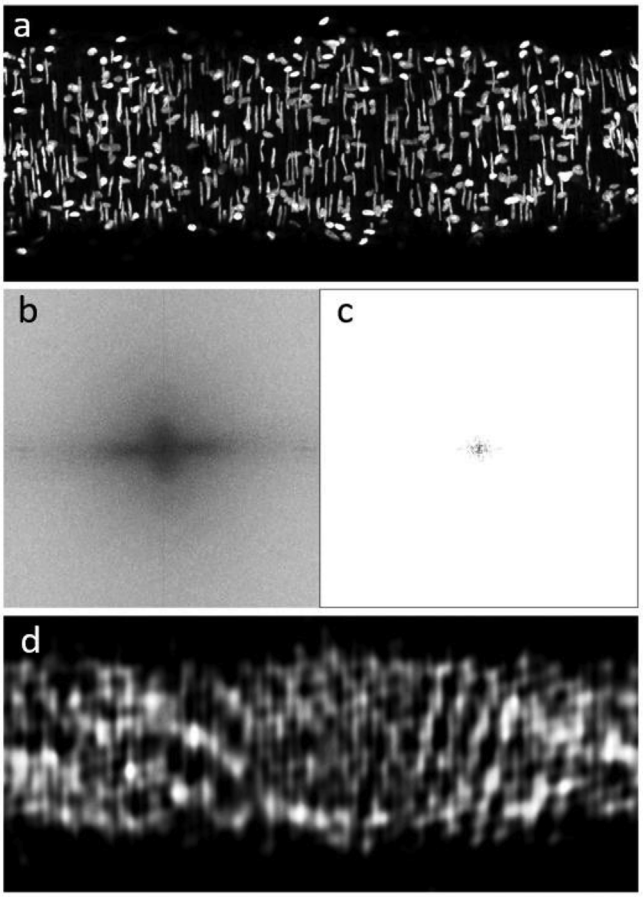

Fig. 5. FFT analysis of mouse mesenteric artery smooth muscle cell arrangement. a) Mouse tail artery segment pressure fixed at 70 mmHg and stained with nuclear fluorescent stain. b) Fast Fourier Transform (FFT) of the image in (a). c) Thresholding selects a small group of low frequency peaks from the FFT in (b). d) Inverse FFT of low frequency peaks in (c) reveals the low frequency patterns in the image.

the angle of the diagonal chain of VSMCs, a reference line was drawn across the length of the artery, following the direction of blood flow. Subsequently, the angle of the diagonal chain of adjacent VSMCs was then measured against the reference line. The angle was measured from the centre point of the VSMC nuclei forming the diagonal chain. The inclusion criteria for the measurements was that the chain had to contain more than four VSMC nuclei aligned as described above. The angle measurements were obtained from the original images, prior to pattern analysis, and then from the inverse FFT images to enable comparison between the angles obtained from both methods.

2.10. Statistical analysis

Minitab 18 (Minitab Ltd, UK) was used for all statistical analysis. The angle values obtained from the Original image and inverse FFT images were analysed using box plots. Furthermore, both data sets were compared in a paired *t*-test to determine if there was significant difference between the overall mean angle obtained from the original image data set and the overall mean angle obtained from the inverse FFT data set.

3. Results

3.1. Vascular structure

Data obtained from previous CLSM studies of vascular structure was used to create a typical 'textbook-style' model of vascular structure (Fig. 1). The 3D model was created in Autodesk Maya and comprises both real and created elements. The perivascular adipocytes surrounding the vessel are from CLSM data as are the adventitial fibroblasts, the internal elastic lamina and the endothelial cells. The white nerve plexus is also modelled from CLSM data. The external elastic lamina is drawn and the tunica media is an artist's impression showing a 'best guess' at the cellular arrangement.

3.2. Vascular smooth muscle cell orientation

A single 840 slice Gatan 3View dataset of a mouse tail artery segment was used to investigate the morphology and orientation of individual smooth muscle cells within the tunica media. The data set measured 154 × 154 × 58.8 μm. The spacing between each slice was 70 nm. The complete dataset was first volume rendered in AMIRA. The view in Fig. 2a shows the internal surface (tunica intima) with endothelial cells running with the longitudinal axis of blood flow (left to right). An accumulation of red blood cells can be seen resting on the endothelial cells. Smooth muscle cells are caught in cross section in the lower left portion of the volume. The cell profiles are elliptical and are commensurate with the expected long flat morphology of smooth muscle cells. However, the cell orientations suggest that the narrow edge of each cell faces the lumen (radial orientation) whilst the flat surface faces the direction of blood flow (i.e. longitudinal orientation,

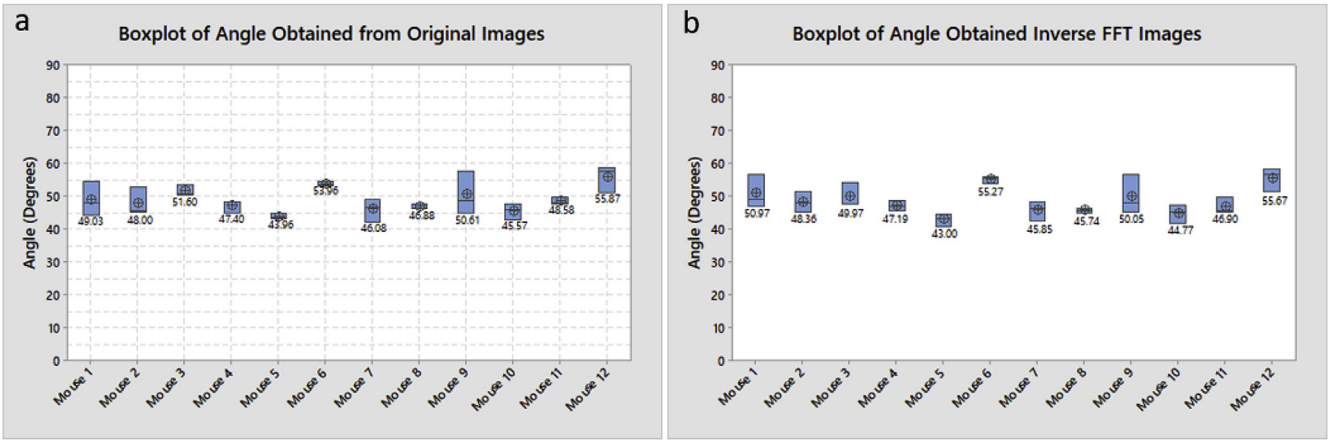

Fig. 6. Analysis of measurements obtained from the original images and inverse FFT images a) Box plot for the angle values obtained from the Original image data set. The mean angle varied from 43.00° to 55.67°. b) Box plot for the angle values obtained from the Inverse FFT image data set. The mean angle varied from 43.96° to 55.87°. Each box represents the mean of 3 data sets.

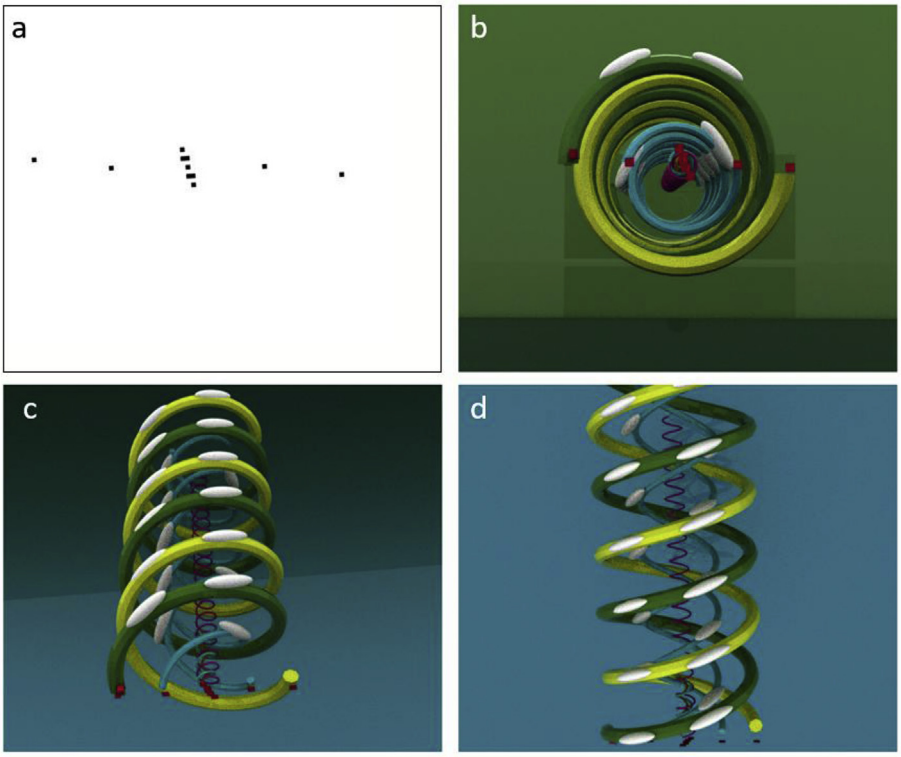

Fig. 7. Generation of 3D sine waves (helices) from low frequency FFT data. a) A group of very low frequency peaks have been isolated from an FFT of an image similar to that shown in Fig. 4 b) Using Autodesk Maya software, the FFT peak distribution was used to determine the amplitude of a series of 3D helices with differing viewpoints shown in (c) and (d). Imagined smooth muscle cell nuclei (in white) have been placed on 3 helices for reference only and without any mathematical basis. The figure is purely theoretical and serves simply to demonstrate the relationship between FFT peaks and possible helical patterns in the data.

the flat surface does not wrap around the lumen). Three individual cells are then isolated by thresholding and segmentation and viewed in relation to the complete volume (Fig. 2b), a single orthoslice depicting the vessel orientation (Fig. 2c) or in isolation (Fig. 2d). A fourth individual smooth muscle cell is isolated and viewed relative to a series of orthoslices to define its true position and orientation (Fig. 2d and f). The flat surface of the cell can be seen to project longitudinally within the wall with the narrow edge projecting towards the luminal (inner) and adventitial (outer) surfaces of the vessel.

3.3. Vascular smooth muscle cell organisation

Mouse mesenteric arteries (36 arteries from n = 12 mice) were stained with a nuclear stain (Syto 61) and membrane stain (DilC18 (3)-DS) and prepared as detailed above. Artery segments were slide mounted and scanned using a Biorad Radiance CLSM. Image collection started just below the external elastic lamina and finished at the beginning of the internal elastic lamina. Images were collected every 0.5 μm through the depth of the tunica media. The image z-series was then combined using an 'average z-projection' process in imageJ software. This results in a single image comprising all medial smooth muscle cells and nuclei. A representative z-projection of a mouse mesenteric artery is shown in Fig. 3. Many of the individual smooth muscle cells have a very narrow appearance and this presumable represents the orientation described above. The cells appear to be organised in bands or groups but that is difficult to quantify. As expected, the cell arrangement (judged by nuclei position) often appear in diagonal sweeps and confirm the general circular arrangement (i.e. right angle to blood flow) of individual vascular smooth muscle cells.

3.4. Quantifying vascular smooth muscle cell organisational patterns using FFT

To investigate the existence of any underlying patterns of smooth muscle cell arrangement in mouse mesenteric arteries, an FFT algorithm was employed via ImageJ. Z-projections were constructed (Fig. 4a) as described above and then segmented to isolate only the cell nuclei in the image (Fig. 4b). The FFT of the segmented image was obtained and lowest frequency peaks were identified (Fig. 4c). The peaks were then used in an 'inverse FFT' transform to create an image of the low frequency patterns within the original image (Fig. 4d). The resulting image has the appearance of a very blurry version of the original that has all of its high frequency detail missing.

The same procedure was carried out on a lower magnification (longer) section of mouse mesenteric artery stained with Syto 61 (Fig. 5a). The FFT (Fig. 5b) and low frequency peaks (Fig. 5c) were then inverse transformed to produce an image of the underlying low frequency pattern (Fig. 5d). When the high frequency detail is removed from the image, underlying patterns are enhanced (compare Fig. 5a and d).

Measurements of the perceived angle of sweeps of smooth muscle cells (diagonal patterning) were made in both the original images and their corresponding inverse-FFTs. The mean angle measured for the original images was 48.96 ± 4.40 the corresponding inverse FFT was measured at 48.65 ± 4.67. Thus, measurements made on both types of image are comparable. This suggestion of a diagonal (helical) arrangement of smooth muscle cells at a pitch of around 49° was used as a guide in the final modelling.

3.5. Statistical analysis of the original image and inverse FFT image data sets

Measurements of apparently diagonal patterns were measured in original and inverse FFT images. The box plot of angles obtained from the original images shows that the mean angle varied from 43.96° to 55.87° (Fig. 6a). The angles obtained from the inverse FFT images ranged from 43.00° to 55.67° (Fig. 6b). This suggests that the angle of the helix varies between 40° and 60° within a range of 0°–90°. Additionally, it was observed that the mean angle of each mouse in both the original image and inverse FFT image data set are similar.

A paired *t*-test was used to compare differences between the overall mean angle obtained from the original image data set (48.96°) and the

overall mean angle obtained from the inverse FFT data set (48.65°). This parametric test was selected due to the normal distribution of both data sets. The test at 95% confidence level returned a p-value > 0.05 and a t-value ≠ zero (p-value = 0.27, t-value = 1.12). Therefore, no significant difference was detected.

3.6. Relationship between low frequency FFT data and helical patterning

A very low frequency set of FFT peaks from a z-projection of mouse mesenteric artery was selected (Fig. 7a) and imported into Autodesk Maya (3D modelling and animation software). The FFT peaks (which exist as symmetrical pairs of points) were used as a guide to create a series of 3D sine waves (helices). The amplitude of the sine waves was guided by the FFT peak pairs (Fig. 7b). The frequency and phase of the waves was estimated for the purposes of the modelling. Two views of the 3D sine waves (helices) are shown in Fig. 7c and d each pair of FFT peaks gives rise to a single coloured helix. Imaginary nuclei are added for reference.

4. Discussion

Vascular remodelling is a prognostic indicator of disease. An increase in small artery wall thickness to lumen diameter ratios (W:L ratio) is well characterised and recognised in hypertension [14]. Furthermore, the remodelling has been attributed to a multitude of factors including, physical forces, transglutaminase, specific integrins, insulin, oxidative stress and inflammation [14]. Whilst vascular remodelling has been widely studied over many decades, knowledge of the development and normal structure of the vascular wall has lagged. A study of the radial development of the pulmonary arterial vessels has implicated platelet derived growth factor-b (PDGF-b) in the initiation of smooth muscle recruitment from inner layers to outer layers [15]. In a review of the dynamic structure of arterioles, Martinez-Lemus provides an excellent diagram of the vascular wall in which a varied orientational pitch of the smooth muscle cells is more realistic than most textbook diagrams [16]. However, whilst representing an excellent short review of vascular cellular connections, no information is given on the organisation of groups of smooth muscle cells or patterns of organisation. The authors of the current study have found that information very difficult to source, particularly for resistance arteries.

Good clues on general vascular structure come from work on porcine aorta [10] and mouse carotid artery [11]. A helical pattern of smooth muscle cell arrangement is suggested to comprise at least two, and perhaps more, right-handed helices. The helix-based modelling is informed by much earlier work in which the muscle in acid-degraded large vessels unwound to form a clear spiral structure [17]. Interestingly Kenneth Strong, in his 1938 paper in the Anatomical Record [17] writes, *'There is little purpose in the exact determination of the angle of the helix because it seems to vary in different vessels and in segments of the same vessel'*. Eighty-one years later we are attempting to measure that angle using FFT analysis and proposing that there is indeed some purpose to it. Simple visual examination of nuclei stained resistance arteries does not reveal any obvious helix (see Figs. 3–5). However, there are aspects of a helical arrangement that suggest its presence. There are also physical characteristics that suggest a spiral or helical structure. Simply increasing the pressure in a mesenteric artery segment causes a marked increase in length. A helical arrangement of smooth muscle cells may facilitate this and thus aid in the pulse wave dampening effects of the small muscular arteries.

Electron microscopy offers the highest resolution of the vascular smooth muscle cell. Using Scanning Electron Microscopy (SEM) it has been shown that individual vascular smooth muscle cells of human cerebral arteries lie in a roughly circular orientation but often have a pitch angle of around ± 35° [18]. That particular SEM study also clearly demonstrates the likelihood of vascular smooth muscle existing as multi-cellular bands, similar to those seen in Fig. 3 of our current report. Whilst the SEM approach provides a 3D-like view of the vessel, it is not possible to extract a single cell for 3D analysis. We have achieved this using a Gatan 3view TEM. The 3D reconstructions clearly show that, in mouse tail artery tunica media, the smooth muscle cells are arranged in a broadly circular fashion with their narrow edge facing down to the lumen (radial alignment) and the flat cell surface aligned longitudinally. Furthermore, careful examination of Fig. 2 suggests that cells lie at a slight pitch angle and are not exactly parallel with the radial axis. In that respect, the diagram of vascular structure presented by Martinez-Lemus [16] is one of the best we have seen. The extremely narrow appearance of the smooth muscle cell cytoplasm of some cells in Fig. 3 can thus be explained by this radial orientation of some cells. We see great value in the use of 3D TEM as a means of extracting highly accurate cellular structures. It should be noted that the individual cells in Fig. 2 exist in a digital format that permits easy 3D printing.

Image transformations are common to many image analysis protocols [18]. The Fast Fourier Transform (FFT) can be used for image compression, smoothing and pattern analysis. The process involves transforming a 2D image from the spatial domain to the frequency domain, altering the frequency domain information and performing an inverse FFT to return to the spatial domain. FFTs are based on the recognition that virtually all signals can be represented as the sum of a collection of sine waves of varying amplitude, frequency and phase. Therefore, an image can be represented as a collection of sine waves. Our aim was to investigate the use of FFTs in determining the lowest frequency sine wave pattern that could represent a helical arrangement of smooth muscle cells. Our approach was to select only the lowest frequency peaks in the FFTs and inverse transform these back to a spatial domain image which could be measured. The rationale being that an image free from high frequency information (visual distractors) could be measured in a more objective way. We measured original images by visually selecting what appeared to be the most obvious helix and then measured the corresponding inverse FFTs that tended to have a more obvious helical appearance (Figs. 4 and 5). Our measurements of both image types were comparable (48.96 vs 48.65°) and indicate that FFT-based measurements could reduce investigator bias and furthermore could be incorporated into a batch process or automated macro within ImageJ. We have found this method to be relatively simple to implement. Whilst not as detailed as a full 3D mathematical modelling approach, we believe that biological scientists, undergraduate student and other non-mathematical specialists could make significant use of this FFT-based approach.

Finally, in order to illustrate the utility of the low frequency FFT peaks, we have modelled one set of points in 3D. Fig. 7a shows four pairs of symmetrical points arrange around a central point. The distance between points in a pair represents the amplitude of a sine wave. Therefore four sine waves can be constructed which, when viewed in 3D, form helices. It is likely that the smallest amplitude helix describes the longitudinal axis of the vessel segment. We have assumed the other three may represent smooth muscle helices. However, it should be stressed that this is purely for illustrative purposes and the amplitude (helix diameter) is the only element that can be relied on. Placing smooth muscle cell nuclei on each of the three main helices is also for illustrative purposes only. Our vision is that this FFT analysis linked with 3D modelling may provide other investigators with ideas on how this type of pattern analysis could be used in other applications.

A limitation of our study is that we have used extended focus views (z-projections) of the vascular wall, thus reducing a 3D volume to a 2D image. We believe that the helical arrangement extends both radially and longitudinally but for the purposes of this study we have ignored the radial dimension. This could, and should, be studied in 3D volumes using orthogonal sectioning.

It is perhaps surprising that, after 120 years of recognition that certain medical conditions are accompanied by vascular remodelling, we still do not have a precise explanation of how vascular cells are normally arranged in small muscular (multi layered) arteries. Every

textbook will describe the 'circular' arrangement of smooth muscle in the tunica media (perpendicular to blood flow) and the flow-related orientation of the endothelial cells (parallel to the blood flow). The scientific literature suggests that vascular smooth muscle has a helical organisation which is perhaps right-handed. The organisation may be a combination of multiple helices (the authors favoured hypothesis). However, the exact organisation of the smooth muscle cells is still not clearly defined for those resistance arteries that are particularly susceptible to remodelling as a result of a hypertensive condition. We believe that a thorough understanding of this basic structure will better inform our interpretation of diseased 'remodelled' vessels.

5. Conclusions

There is no doubt that vascular smooth muscle adopts some form of helical arrangement. The number of helices and their relative pitch probably varies with vessel diameter, function and species. In mouse mesenteric arteries we suggest that there is at least one underlying helix which has a pitch angle of around 49°. This hypothesis can now be tested and examined by others. Furthermore, we propose that a simple FFT-base image analysis method is suitable for further studies in this important area of vascular research. It will be of interest to use FFT-based analysis to compare healthy and diseased (remodelled) arterial structure.

Acknowledgements

The authors are grateful to Uti Sari and Catherine MacRobbie for their contributions to the construction of the vascular model in Fig. 1. We are also extremely grateful to Dr David I Hughes and Professor Andrew Todd for providing access to their CLSM.

References

[1] W.W. Gull, H.G. Sutton, Chronic Bright's disease with contracted kidney, Medico-Chirurgical Transactions, 1872, 55 1872, pp. 273–326.
[2] D. Short, Morphology of the intestinal arterioles in chronic human hypertension, Br. Heart J. 22 (1966) 184–192.
[3] G.L. Baumbach, Heistad, Remodeling of cerebral arterioles in chronic hypertension, Hypertension 13 (1989) 968–972.
[4] M. Mulvany, Vascular remodelling of resistance vessels: can we define this? Cardiovasc. Res. 41 (1) (1999) 9–13.
[5] J.R. Levick, An Introduction to Cardiovascular Physiology, fifth ed., Hodder Arnold, 2010.
[6] A. Nakano, M. Minamiyama, J. Seki, The three-dimensional structure of vascular smooth muscle cells: a confocal laser microscopic study of rabbit mesenteric arterioles, Asian Biomed. 1 (1) (2007) 77–86.
[7] M.E. Todd, C.G. Laye, D.N. Osborne, The dimensional characteristics of smooth muscle in rat blood vessels, Circ. Res. 53 (1983) 319–331.
[8] C.J. Daly, A. McGee, E. Vila, A. Briones, S.M. Arribas, S. Pagakis, J. Adler, A. Merle, J. Maddison, J. Pedersen, J.C. McGrath, Analysing the 3D structure of blood vessels using confocal microscopy, November, Micros. Anal. 92 (2002) 5–8.
[9] J.C. McGrath, C. Deighan, A.M. Briones, M.M. Shafaroudi, M. McBride, J. Adler, S.M. Arribas, E. Vila, C.J. Daly, New aspects of vascular remodelling: the involvement of all vascular cell types, Exp. Physiol. Jul. 90 (4) (2005) 469–475.
[10] Z. Tonar, P. Kochova, R. Cimrman, J. Perktold, K. Witter, Segmental differences in the orientation of smooth muscle cells in the tunia media of porcine aortae, Biomechanics Model. Mechanobiol. 14 (2015) 315–332.
[11] B. Spronck, R.T.A. Megens, K.D. Reesink, T. Delhaas, A method for the three-dimensional quantification of vascular smooth muscle orientation: application in viable murine carotid arteries, Biomech. Model. Mechanobiol. 15 (2016) 419–432.
[12] Haahr, M. and Haahr, S. (1998). (Random.org [online]).
[13] C.-M. Hai, Vascular Smooth Muscle: Structure and Function in Health and Disease, 1 ed., World Scientific Publishing Company, 2016, pp. 213–238 [ebook] Singapore.
[14] E. Agabiti-Rosei, D. Rizzoni, Microvascular structure as a prognostically relevant endpoint, J. Hypertens. 35 (5) (2017) 914–921.
[15] D.M. Greif, M. Kumar, J.K. Lighthouse, J. Hum, A. Anadrew, L. Ding, K. Red-Horse, F.H. Espinoza, L. Olson, S. Offermanns, M.A. Krasnow, Radial construction of an arterial wall, Develop. Cell 23 (2012) 482–493.
[16] L.A. Martinez-Lemus, The dynamic structure of arterioles, Basic cpharmacol. Toxicol. 110 (0) (2012) 5-11. 1742-7843.
[17] K.C. Strong, A study of the structure of the media of the distributing arteries by the method of microdissection, Anat. Rec. 72 (1938) 151–168.
[18] J.C. Russ, F.B. Neal, Processing images in frequency space, The Image Processing Handbook, seventh ed., CRC Press. Taylor & Francis group, 2016.